Proceedings of the 8th International Conference on Energy Harvesting, Storage, and Transfer (EHST 2025)
July 15, 2025 - July 17, 2025 | Imperial College London Conference, London, United Kingdom
Paper No. 116
DOI: 10.11159/ehst25.116

Thermodynamic And Mechanical Measurement Of The Flow Of A Vaporized Fluid In A Cylinder: The Case Of The Atmospheric Distillation Of Crude Oil.

Ndiassé FALL[1*], Dialo DIOP[1], Haroun Ali ADANNOU[2], Kharouna TALLA[1]
[1]Solid State Physics ad Materials Science Laboratory Group, Faculty of Science and Technology, Cheikh Anta Diop University of Dakar, Dakar, Senegal.
[*] fallndiasse93@gmail.com, dialo.diop.ucad@gmail.com,
kharouna.talla@ucad.edu.sn
[3]Chemical Engineering Département, Mao National Higher Petroleum Institute, Mao, Tchad.
harounali100@gmail.com

***Abstract* –** During atmospheric distillation after injection of the previously vaporized oil into the furnace, the rise of steam in the column generates heat and mass transfer phenomena.
The aim of this article is to study the thermal conduction in the column in order to determine theoretically the thermal resistance of the different oil cuts as well as the heat released in each cut that will later be used to heat the crude.
But also, to study, using the Navier–stokes equation, the rise of vapours along the cylindrical column as well as the velocity and pressure fields of the vapours in the column.
This study showed that after injection the temperature in the column decreases considerably as well as the heat flux as the steam progresses through the column despite almost zero thermal resistance.
The results also showed that the pressure of the vaporized crude varies slightly with increasing flow velocity. On the other hand, the flow velocity within the cylinder is very little influenced by pressure.
The interest of this study of heat and mass transfer phenomena will later be used to evaluate and then quantify certain notions depending on the temperature, pressure or flow velocity of the fluid such as corrosion within the column as well as energy management techniques in thermal industries and in the management of industrial equipment.

Nomenclature
C: Mass heat capacity of the material ($J.Kg^{-1}.k^{-1}$).
g: Intensity of gravity ($m.s^{-2}$).
(h_1..........h_n) : Thermal convection coefficients from 1 to n ($W.m^{-2}.K^{-2}$).
K: Thermal conductivity ($W.m^{-1}.K^{-1}$).
P: pressure (Pa).
P_1............... P_n: Tray 1 to n.
Pth: Thermal energy density ($W.m^{-3}$).
Rcv1............... Rcvn: Convection thermal resistance from medium 1 to medium n ($W^{-1}.K$).
Rcd: Conduction thermal resistance ($m.W^{-1}.K$).
S: Surface area of a tray (m^2).
T_1......... T_n: Temperature 1 up to temperature n (K).
T'_1 .... T'_n : Temperature 1 up to a temperature n "ends of the trays" (K).
T_p : Temperature of a tray (K).
V: Fluid velocity ($m.s^{-1}$).
Greek Letters:
$\overrightarrow{\varphi_1} \dots\dots \overrightarrow{\varphi_n}$: Heat flux density vector 1 up to n ($W.m^{-2}$).
$\emptyset_{m1}$...............$\emptyset_{mn}$: Heat flux from medium 1 to medium n ($W.k^{-1}$).
ρ : Density ($Kg.m^{-3}$).
ω: Angular velocity ($rad.s^{-1}$).
μ : Dynamic viscosity ($Kg.m^{-1}.s^{-1}$).

***Keywords*:** flow velocity - heat flow- pressure - temperature - thermal resistance.

1. Introduction

Heat and mass exchanges phenomena are observed in various industries.

However, if left unchecked, these phenomena can have disastrous consequences in terms of material life and safety within these industries.

In applied physics, the determination of thermal and mass exchanges, as well as the flow velocity of fluids, is very useful in the study of turbulence and corrosion of materials.

This study involves using physical and computational tools to characterize and then quantify heat and mass exchanges, as well as the pressure and flow velocity of fluids within the atmospheric distillation column of crude oil.

In the literature, many authors have worked on the measurement of heat and mass exchanges and the phenomena that can impact these exchanges, including thermal resistance and possible physical factors.

P. P. Singh and D. E. Maier **[1]** have demonstrated by simulation that hot spots arise due to the flow of heat in three dimensions from the source to the roller ends and the curved surface. But also, an estimated heat flux value of 56 kW/m^2 gave surface temperature values close to the observed values. Perturbations of the baseline values showed that a 10% increase in thermal conductivity caused a 6-8% reduction in the peak thermal gradient, whereas a 20% increase in the heat transfer coefficient caused less than 2% reduction in the peak thermal gradient therefore, thermal conductivity is a more sensitive parameter affecting thermal gradients than the heat transfer coefficient. It is extremely difficult to obtain an analytical solution when the heat flow travels along a curved surface and convection takes place at the ends of a roller. In such cases, the use of the digital method becomes essential. Ootao et al. **[2]** performed a theoretical analysis of a three-dimensional transitive thermal tension problem for a non-homogeneous circular cylinder subjected to a moving heat source in the inner axial direction and/or the outer surface. A mass balance approach was employed to analyse the effect of nanoparticle migration on laminar convection and proposed that shear forces and viscosity gradient induce the motion of nanoparticles will change the distribution and thus vary the viscosity and thermal conductivity of the fluid [3**].** The increase in the heat transfer coefficient did not decrease the peak temperature to a smaller portion of the curved surface. The disturbance resulted in a 0.5°C decrease in peak temperature but less than 2% variation in thermal gradient value, indicating that surface heat transfer coefficient is a less sensitive parameter than thermal conductivity in affecting thermal gradients and high-temperature corrections [1].

In thermal conduction oils and gases can be considered as thermal resistances to heat conduction [4].

The effective thermal resistance (or thermal conductivity) of the heat pipe is one of the most important parameters and is not constant but is a function of a large number of variables, such as the geometry of the heat pipe, the length of the evaporator and condenser, and the nature of the fluid in question [5**].** The total thermal resistance of a heat pipe is the sum of the resistances due to conduction through the wall (heat pipe casing) and the wick, evaporation or boiling, axial steam fluid, condensation, and conduction losses through the wick, in the condenser and heat pipe. The heat flux depends on the distance between the condenser area and the evaporator, the overheating of the walls and the subcooling of the liquid, the thermal contact between the heater and the wick, and the conditions at the surface boundaries of the wick [5].

The internal heat source by viscous dissipation and the temperature-dependent heat source increases the temperature of the fluid, thus decreasing the temperature difference between the fluid and the heated plate, hence the observed decrease in heat transfer on the heated plate [6**].**

The use and examination of mass transfer resistances in the process domain is an effective method to understand the process and identify ways to improve it [7].

The studies of Schaaf et al. and Chiekar et al. [8,9] on the gas-liquid mass transfer in a 0.15m diameter bubble column with a pressure of 0.1 to 1.3 MPa and presented the correlation of the mass transfer coefficient.

Analysis of Prantl numbers shows that velocity fields decrease while temperature distributions increase [10].

To study heat fluxes and heat transport mechanisms in structured reactors, it is more convenient to use the numerical method of fluid dynamics [11].

The simulation allows to efficiently study the three mechanisms of heat transfer: conduction, convection and radiation in open-cell foams but also other influencing parameters such as surface velocity, wall coupling, thermal conductivity and geometric influence on heat transport [12-20].

The objective of this article is to characterize the phenomena of heat transfer and mass but also to evaluate the pressure and flow velocity of the fluid within the atmospheric distillation column in order to better maintain refining equipment and in industries with the same operating principle.

The rest of this article is divided into three parts. We will first define the materials and methods used and then present and discuss the results obtained before summarizing them and giving the perspectives of this study.

2.Material and method:

2.1. Material:

The study is carried out by modelling the atmospheric distillation column with cylindrical geometry.

In the models defined, we will adopt the equations of the fourrier's law and the continuity of heat flows, in particular conduction and convection, in order to determine the equation of temperature, heat quantities and finally the thermal resistances characteristic of this type of flow.

For the mass transfer, the Navier-Stockes equation will be applied to this study in order to determine the characteristic pressure and velocity of this flow.

In the study of mass and heat transfer phenomena, the difficult access to equipment makes it more convenient to use a computational or numerical method rather than experimental methods.

After defining the characteristic equations for this model, we will use computer programming to model them and obtain the results of this study.

2.2. Method:

2.2.1. Study of thermal conduction in the atmospheric distillation column: theoretical determination of the thermal resistance and heat exchange:

The atmospheric distillation column is a vertical cylindrical device with a height of between 40 and 50 m, it is equipped with horizontal partitions called trays whose role is to ensure intimate contact between the liquid and the vapor in order to allow the balance of the phases following the transfer of heat and materials. However, this after heating the crude oil and injecting it into the column; The constituents of the crude oil previously heated in the furnace are dispersed in the horizontal column in the form of vapours.

Each tray has a temperature that decreases as you go up the column.

There is a heat transfer phenomenon that takes place throughout the column; Each tray is placed between two fluids of different temperatures.

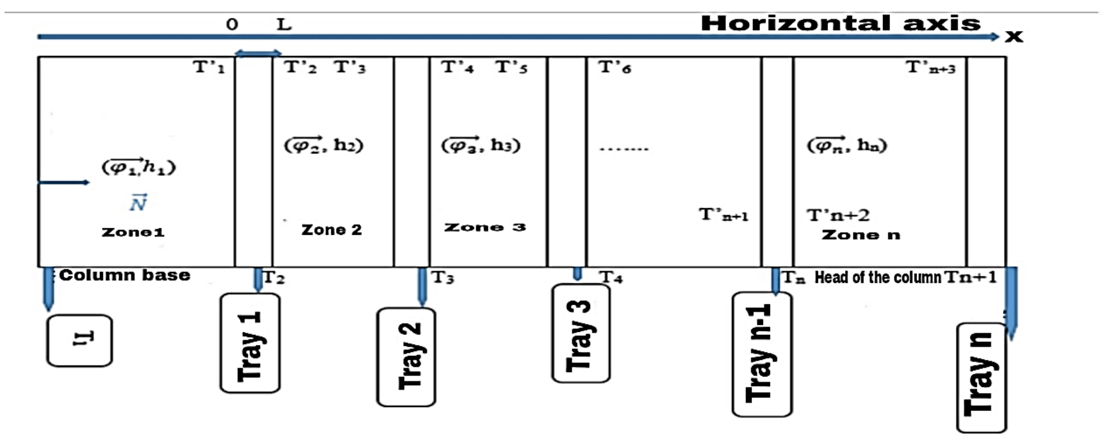

Figure 1: Simplified representation of the spatial and thermal dimensions of an atmospheric distillation.

The flux density vector in each section is given by:

$\overrightarrow{\varphi_1} = h_1 (T_1 - T'_1)\vec{N}$ (1) ; $\overrightarrow{\varphi_2} = h_2 (T'_2 - T'_3)\vec{N}$ (2); $\overrightarrow{\varphi_3} = h_3 (T'_4 - T'_5)\vec{N}$ (3) ………… $\overrightarrow{\varphi_n} = h_n (T'_n - T'_{n+1})\vec{N}$ (4) n = 2……..∞.

NB: if the tray is thin enough, then: $T'_n = T'_{n+1} = T_n$: n=2………∞ ; $T'_1 = T_2$.

2.2.1.1 Study of the heat balance in the column:

According to the law of variation of the internal energy of the system:

$$\iiint \boldsymbol{p_{th} d_v} = \iiint \boldsymbol{\rho c \frac{\partial T}{\partial t} dV} - \iint \boldsymbol{K \overrightarrow{grad}\, T} \text{ ds } \mathbf{(5)}$$

According to Green Ostrogratsky's theorem:

$$\iiint \boldsymbol{p_{th} d_v} = \iiint \boldsymbol{\rho c \frac{\partial T}{\partial t} dV} - \iiint \boldsymbol{div\ (k \overrightarrow{grad}\, T) dv} \ \mathbf{(6).}$$

The integration limits being any:

$$\mathbf{P_{th}} = \boldsymbol{\rho c \frac{\partial T}{\partial t}} - \text{div } (\text{k}\overrightarrow{grad}\text{T}) \ \mathbf{(7)}.$$

K being uniform in the trays of the column:

$$\mathbf{P_{th}} = \boldsymbol{\rho c \frac{\partial T}{\partial t}} - \mathbf{k}\Delta \boldsymbol{T} \ \mathbf{(8)}$$

With:

P_{th}: Thermal energy density.

$\boldsymbol{\rho c \frac{\partial T}{\partial t}}$ **:** term of exchange.

KΔT : term for thermal energy storage.

In our study there is no energy production at the spine level, energy exchanges with the external environment are also negligible.

So, the equation becomes:

$$\Delta T = 0 \ \mathbf{(9)}$$

$$\frac{\partial^2 T}{\partial^2 x^2} = 0 \quad \Rightarrow \quad \frac{\partial T}{\partial x} = A \Rightarrow T(x) = Ax + B$$

Boundary Conditions **:** **X=0 => T (0) = T'$_1$=B**

X=L => T(L)=T'$_2$= AL +T'$_1$ => A = $\frac{T'_2 - T'_1}{L}$

$$T_p(x) = \left[\frac{T'_2 - T'_1}{L}\right] x + T'_1 \quad \mathbf{(10)}$$

This equation is valid in a tray only if it is of a thickness L.

Otherwise: **x=0 and $T_p(0)=T_2=T'_1$.**

2.2.1.2. Study of the evolution of the temperature parameter of the steam:

2.2.1.2.1. Determination of temperature equations:

Based on the continuity of the heat flow:

In medium 1 we have:

$$-k\frac{dT}{dx} = h_1 (T_1 - T'_1) \Rightarrow T_{m1}(x) = \frac{h_1}{k}(T'_1 - T_1)\, x + A \text{ or } T_{m1}(0) = T'_1$$

$$\text{Then: } T_{m1}(x) = \frac{h_1}{k}(T'_1 - T_1)\, x + T'_1 \ \mathbf{(11)}$$

In the medium 2:

$$-k\frac{dT}{dx} = h_2 (T'_2 - T'_3) \quad \Rightarrow T_{m2}(x) = \frac{h_2}{k}(T'_3 - T'_2)\, x + B \quad \text{or } T_{m2}(L) = \frac{h_2}{k}(T'_3 - T'_2)\, L + B = T'_2$$

As a result, **$B = T'_2 - \frac{h_2}{k}(T'_3 - T'_2)\, L$** so **$T_{m2}(x) = \frac{h_2}{k}(T'_3 - T'_2)\, x + T'_2 - \frac{h_2}{k}(T'_3 - T'_2)\, L = \frac{h_2}{k}(T'_3 - T'_2)(x - L) + T'_2$**

$$T_{m2}(x) = \frac{h_2}{k}(T'_3 - T'_2)(x - L) + T'_2 \ \mathbf{(12)}$$

2.2.1.3. Determination of heat flux and densities:

In the medium 1:

The flow is given by the relation $\emptyset = \iint \vec{\varphi}\ \vec{ds}$

Where $\boldsymbol{\varphi_{m1} = -k\frac{dT_{m1}(x)}{dx}}$**= h₁ (T₁– T'₁)** **=>** $\emptyset_{m1}$**= h₁ (T₁– T'₁) S**

$$\emptyset_{m1} = h_1 (T_1 - T'_1)\, S \quad (13)$$

For the tray:

$\boldsymbol{\varphi_p = -k\frac{dT_p(x)}{dx}}$ **= k** $\left[\frac{T'_1 - T'_2}{L}\right]$

$$\emptyset_p = k\left[\frac{T'_1 - T'_2}{L}\right] S \quad (14)$$

For the medium 2:

$\boldsymbol{\varphi_{m2} = -k\frac{dT_{m2}(x)}{dx}}$**= h₂ (T'₂– T'₃)** **=>** $\emptyset_{m2}$**= h₂ (T'₂– T'₃) S**

$$\emptyset_{m2} = h_2 (T'_2 - T'_3)\, S \quad (15)$$

For any medium:

$$\emptyset_{mn} = h_n (T'_n - T'_{n+1})\, S \quad (16)$$

n = 2………………∞ **S**: the surface of the tray.

NB: The flux of the medium n (oil cut) is the amount of heat released by this cut; This heat will be recovered after cooling the corresponding cut and then used to heat the crude.

2.2.1.4. Determination of thermal resistance in the trays and at the oil cuts:

By electrical correlation we have:

For the medium 1:

$$\emptyset_{m1} = \frac{\Delta T}{R_{cv1}} = \frac{(T1 - T'1)}{\frac{1}{Sh_1}}$$

By identification, the convection resistance of medium 1 is**:**

$$R_{cv1} = \frac{1}{Sh_1} \quad (17)$$

For the medium 2:

$$\emptyset_{m2} = \frac{\Delta T}{R_{cv2}} = \frac{(T'2 - T'3)}{\frac{1}{Sh_2}}$$

By identification the convection resistance of the medium 2 is:

$$R_{cv2} = \frac{1}{Sh_2} \quad (18)$$

For a medium n the thermal resistance of convection is:

$$R_{cvn} = \frac{1}{Sh_n} \quad (19)$$

NB: thermal resistance R_{cvn} in reality the thermal resistance of the n oil cuts constituting the column.

For the tray:

The $\emptyset_p$ of a tray is given by :

$$\emptyset_p = k\left[\frac{T'_1 - T'_2}{L}\right] S = \frac{\Delta T}{R_{cd}} = \frac{\Delta T}{\frac{L}{KS}}$$

$$R_{cd} = \frac{L}{KS} \quad (20)$$

R_{cd}: Conduction resistance of the plate, K: Thermal conductivity of a plate.

2.2.2. Dynamic study of the steam rise, determination of the velocity and pressure of the fluid:

A distillation column is a cylinder through which a heavy, viscous vapour rises from the base to the head of the column.

In this section, we propose to study mass transfer using the Navier-stokes equation to determine the velocity and pressure fields.

This rise is all the more important thanks to the stripping steam injected at the bottom of the column to first vaporize the heavy molecules contained in the atmospheric residue but also to promote the rise of the vapor contained in the column.

The rising steam is assumed to have an angular velocity (ω).

To study the velocity and pressure field, we make a theoretical study on the upward flow of two distinct vapours contained in two coaxial cylinders and which have the respective radius and angular velocities: $(\omega_1, R_1), (\omega_2, R_2)$.

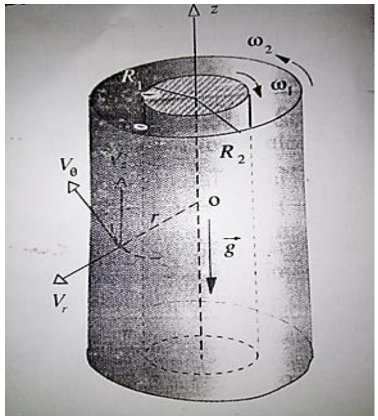

Figure 2: Representation of the cylindrical coordinates of the atmospheric distillation column **[21].**

The Navier-Stokes equation gives**:**

$$\boldsymbol{\rho}\left[\frac{\partial\vec{v}}{\partial t} + (\vec{v}\overrightarrow{grad})\vec{v}\right] = -\overrightarrow{grad}\mathbf{P} + \mu\Delta\vec{v} + \rho\vec{g} \ \textbf{(21)}$$

$$\vec{v} = \vec{v}(r, \theta, z)$$

The motion is assumed to be permanent $\frac{\partial}{\partial t} \equiv 0$ and revolutionarily symmetrical according to θ the unknown functions of the flow field are: v_r **(r, z) ;** v_θ**(r, z) ;** v_z**(r, z) ; P(r, z)**

Using the cylindrical coordinates we obtain:

For $(\vec{v}\overrightarrow{grad})\vec{v}$ **:**

$(\vec{v}\overrightarrow{grad}) = (v_\theta\vec{e_\theta})\left(\frac{1}{r}\frac{\partial}{\partial\theta}\vec{e}_\theta\right)$ **;** $v_z \cong \mathbf{0}$ Because the rotational flow is much greater: the size of the column is very large in relation to its radius.

$$\vec{v}\overrightarrow{grad} = \frac{v_\theta}{r}\frac{\partial}{\partial\theta} \ \textbf{(22)}$$

$$(\vec{v}\overrightarrow{grad})\vec{v} = \frac{v_\theta}{r}\frac{\partial(v_\theta\vec{e_\theta})}{\partial\theta} = -\frac{v^2}{r}\vec{e}_r \ \textbf{(23)}$$

For $\overrightarrow{grad}P$ **:**

$$\overrightarrow{grad}P = \frac{\partial P}{\partial r}\vec{e}_r + \frac{1}{r}\frac{\partial P}{\partial\theta}\vec{e}_\theta + \frac{\partial P}{\partial z}\vec{e}_z \textbf{(24)}$$

For: $\Delta\vec{v}$

$\Delta\vec{v} = \overrightarrow{grad}$ **(div**$\vec{v}$ **)-**$\overrightarrow{rot}(\overrightarrow{rot}\vec{v})$ **in wich div** $\vec{v}$**=0** because the fluid is incompressible**.**

$$\overrightarrow{rot}\vec{v} = \overrightarrow{rot}(v\overrightarrow{e_\theta}) = v\overrightarrow{rot}\vec{e}_\theta + \overrightarrow{grad}v \wedge \vec{e}_\theta = \frac{v}{r}\vec{e}_z + \frac{\partial v}{\partial r}\vec{e}_z = \frac{1}{r}\left[v\frac{\partial r}{\partial r} + r\frac{\partial v}{\partial r}\right]\vec{e}_z$$

$$\overrightarrow{rot}(\overrightarrow{rot}\vec{v}) = \overrightarrow{rot}\left[\frac{1}{r}\left[v\frac{\partial r}{\partial r} + r\frac{\partial v}{\partial r}\right]\vec{e}_z\right] = \overrightarrow{grad}\left[\frac{1}{r}\left[v\frac{\partial r}{\partial r} + r\frac{\partial v}{\partial r}\right]\right] \wedge \vec{e}_z = \frac{\partial}{\partial r}\left[\frac{1}{r}\left[v\frac{\partial r}{\partial r} + r\frac{\partial v}{\partial r}\right]\right]\vec{e}_r \wedge \vec{e}_z$$

$$= -\frac{\partial}{\partial r}\left[\frac{1}{r}\left[v\frac{\partial r}{\partial r} + r\frac{\partial v}{\partial r}\right]\right]\vec{e}_\theta = -\frac{\partial}{\partial r}\left[\frac{1}{r}\frac{\partial}{\partial r}(r.v)\right]\vec{e}_\theta$$

$$\Delta\vec{v} = \frac{\partial}{\partial r}\left[\frac{1}{r}\frac{\partial}{\partial r}(r.v)\right]\vec{e}_\theta \textbf{(25)}$$

If we project the Navier-stokes equation:
According to r we have:

$$-\frac{\rho v^2}{r} = -\frac{\partial P}{\partial r} \quad (26)$$

According to θ

$$:\frac{-1}{r}\frac{\partial P}{\partial \theta} + \mu\frac{\partial}{\partial r}\left[\frac{1}{r}\frac{\partial}{\partial r}(r.v)\right] = 0 \quad \mathbf{(27)}$$

According to z:

$$-\frac{\partial P}{\partial z} - \rho g = 0 \quad \mathbf{(28)}$$

The integration of the equation in z axis gives:

P (r, z) = $-\rho g z + f(r)$ (29) Where the function f(r) of the radial distance remains to be determined. We can already conclude that on any circular cylinder r = constant; The expression obeys a law of hydrostatic distribution according to the vertical.

Introducing this result into the equation following r we deduce that:

$$v^2{}_\theta = \frac{r}{\rho}\frac{df}{dr} \quad \mathbf{(30)}$$

Which shows that the component is only a function of r. In the following, and to lighten we have: $v_\theta(r) = v(r)$**.**

The following equation according to the component θ gives:

$$\frac{d}{dr}\left[\frac{1}{r}\frac{d}{dr}(r.v)\right] = 0 <=> \frac{dv}{dr} + \frac{v}{r} = A \quad \mathbf{(31)}$$

2.2.2.1. Calculation of the velocity field:

If we consider two ascending steam vortices of respective radius and angular velocities (R_1, ω_1) ;(R_2, ω_2) we have after integration:

$$v(r) = \frac{A}{2}r + \frac{B}{r} \quad (32)$$

$A = \frac{2\omega_2 R_2{}^2 - \omega_1 R_1{}^2}{R_2{}^2 - R_1{}^2}$ $B = (\omega_1 - \omega_2)\frac{R_1{}^2 R_2{}^2}{R_2{}^2 - R_1{}^2}$

2.2.2.2. Calculation of the pressure field:

We have according to equation (30):

$$v^2{}_\theta = \frac{r}{\rho}\frac{df}{dr} => \frac{df}{dr} = \rho\left[\frac{A^2 r}{4} + \frac{AB}{r} + \frac{B^2}{r^3}\right] \quad \mathbf{(33)}$$

The integration gives:

$$f(r) = \rho\left[\frac{A^2 r^2}{8} + ABln(r) - \frac{B^2}{2r^2}\right] + P_0 \quad \mathbf{(34)}$$

Where P_0 is a fixed pressure reference (atmospheric pressure). The definitive expression of the pressure field is:

$$P(r,z) = P_0 - \rho g z + \rho\left[\frac{A^2}{8}r^2 + ABln(r) - \frac{B^2}{2r}\right] \quad \mathbf{(35)}$$

If we apply these results to our distillation column containing a single ascending steam that contains all the vaporized hydrocarbons. The steam has a radius of vortex R and angular velocity, so we have a viscous fluid contained in a circular column in which, it is set in motion of rotation in this column and around its axis.

For this situation we have **A = 2** ω **et B =0,** the velocity field therefore follows a linear growth law

;

$$v = r\omega \quad \mathbf{(36)}$$

The pressure-velocity relationship is therefore expressed by: $P - \frac{1}{2}\rho v^2 + \rho g z = k$ **(37).**

The components of the rotational vector are $\Omega_r = \Omega_\theta = 0$ **;** $\Omega_z = \omega$, it is therefore uniform throughout the fluid **[19].**

For the numerical study of the phenomena described, we have taken specific numerical values compatible with the study conditions.

The thermal conductivity of carbon steels will be considered in this study, the value of which is K= 3650.254 $W.m^{-1}. K^{-1}$.

The value of the convection coefficient for forced convection of oils is between 50 and 2000 $W.m^{-2}.K^{-1}$, we will take h= 1000 $W.m^{-2}.K^{-1}$ for this study.

For the thickness of the plates, L= 0.5 m will be taken for this study.

3. Results and discussions:

3.1. Results

3.1.1. Temperature distribution on a tray:

Equation (10) shows through Figure 3 representing the longitudinal distribution of temperature on a plate shows that it decreases considerably from the base to the head of the column. In other words, the trays cool from the base to the head of the atmospheric distillation column.

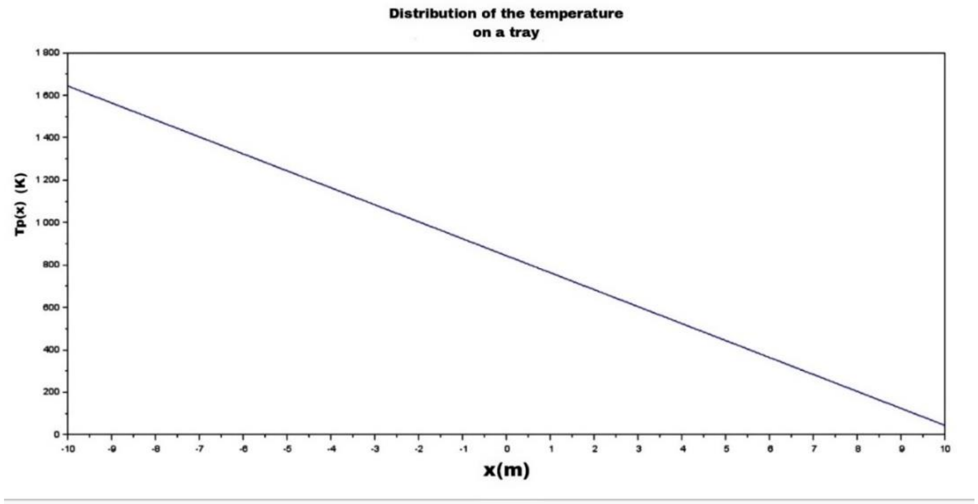

Figure 3: Longitudinal distribution of temperature on a tray.

3.1.2. Distribution of the steam temperature along the column:

Equation (11) shows through Figure 4 representative of the longitudinal evolution of the temperature in the base of the column shows that it decreases considerably.

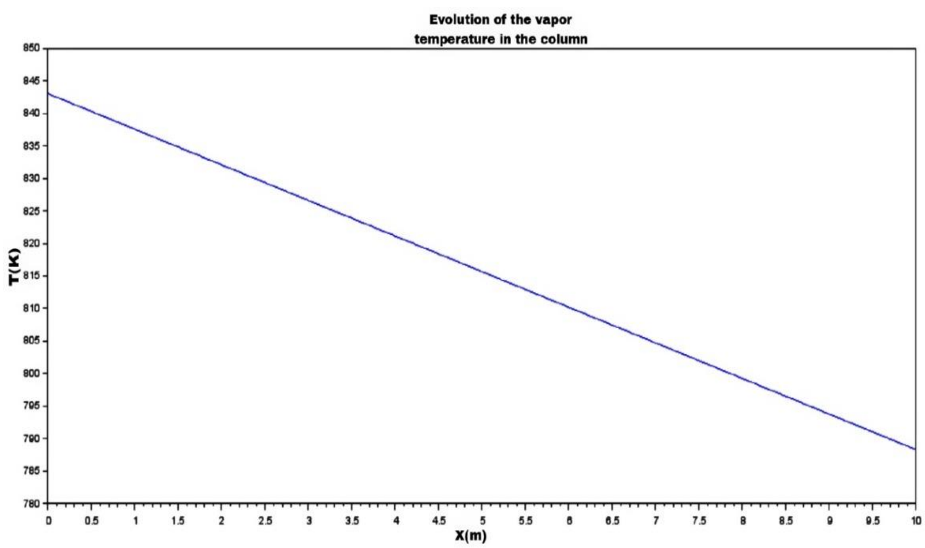

Figure 4: Distribution of the steam temperature along the column

3.1.3. The heat flow exchanged in the column:

Equation (13) representing the heat flux as a function of the surface shows through Figure 5 that it decreases considerably along the column like temperature. This drop in heat flow is due to the reduction in the temperature of the vapors rising towards the head of the atmospheric distillation column.

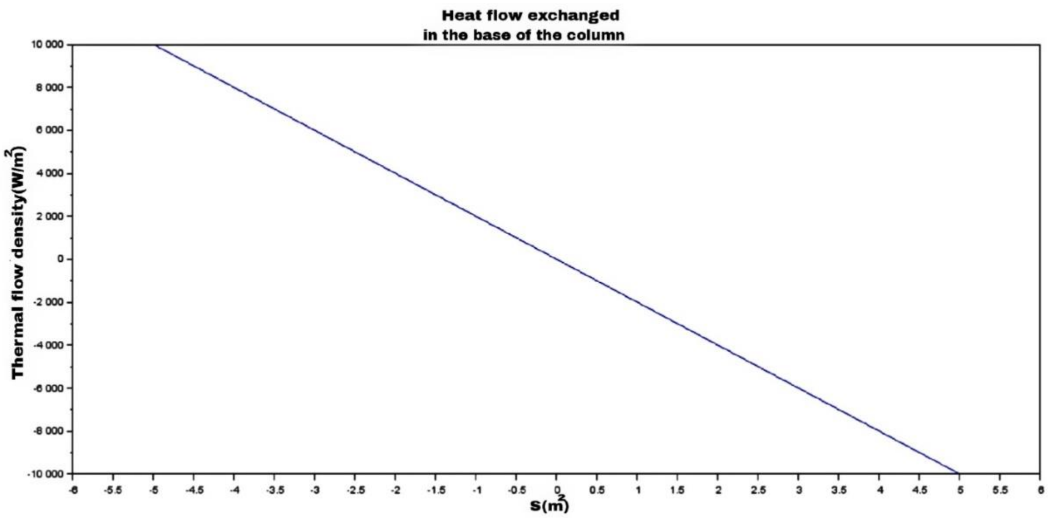

Figure 5: **Evolution** of the heat flux as a function of the surface of the flow.

3.1.4. The thermal resistance of the fluid in the column:

Equation (17) shows through Figure 6 a very low thermal resistance of the vaporized fluid. In fact, vapors have very low thermal resistance.

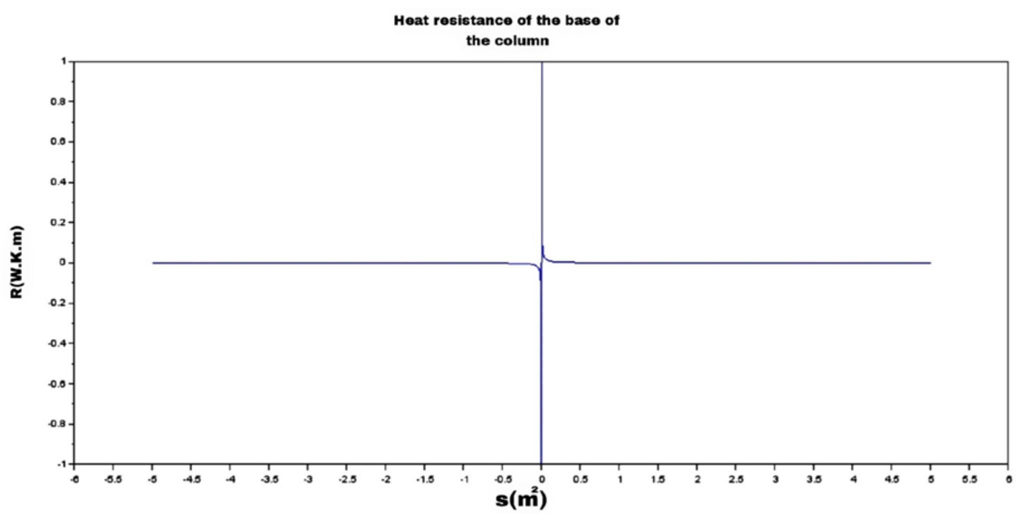

Figure 6: evolution of the thermal resistance of vaporized crude oil

3.1.5. The evolution of the pressure as a function of the flow velocity and the height of the column:

Equation (37) allows us to obtain through Figure 7 the evolution of the fluid pressure in this study, which decreases slightly as a function of the fluid velocity and increases considerably as a function of the height of the column. The pressure of the vaporized crude increases as it rises towards the head of the atmospheric distillation column, regardless of its speed during this rise.

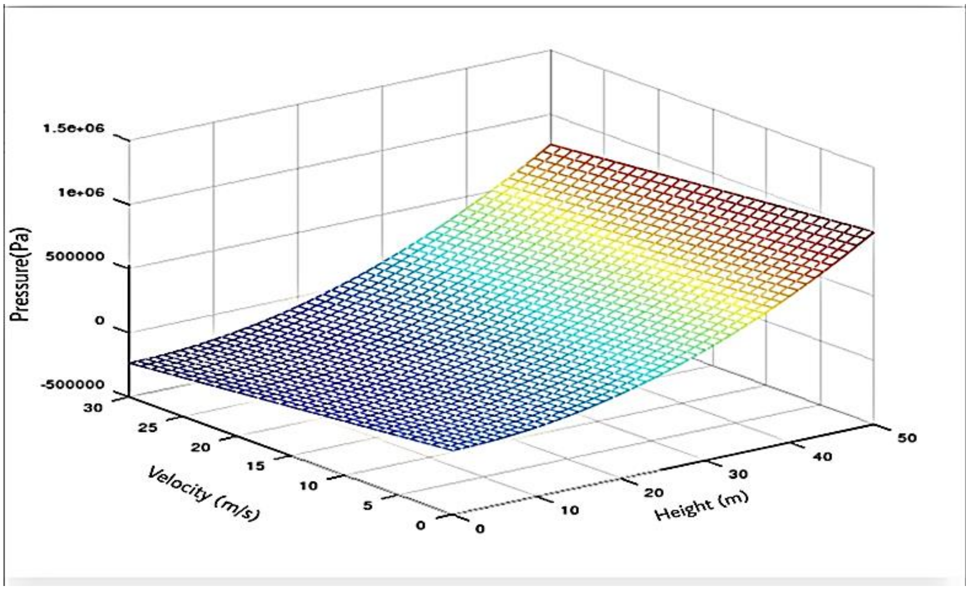

Figure 7: Evolution of the **fluid** pressure as a function of the velocity and height of the column.

3.1.5. The evolution of the fluid velocity as a function of the pressure and the height of the column:

Equation (37) allows us to obtain through Figure 8 the evolution of the square of the velocity which increases considerably with the height of the column and hardly changes with the pressure of the fluid. The velocity of the steam as it rises towards the heat of the column increases considerably and independently of its pressure.

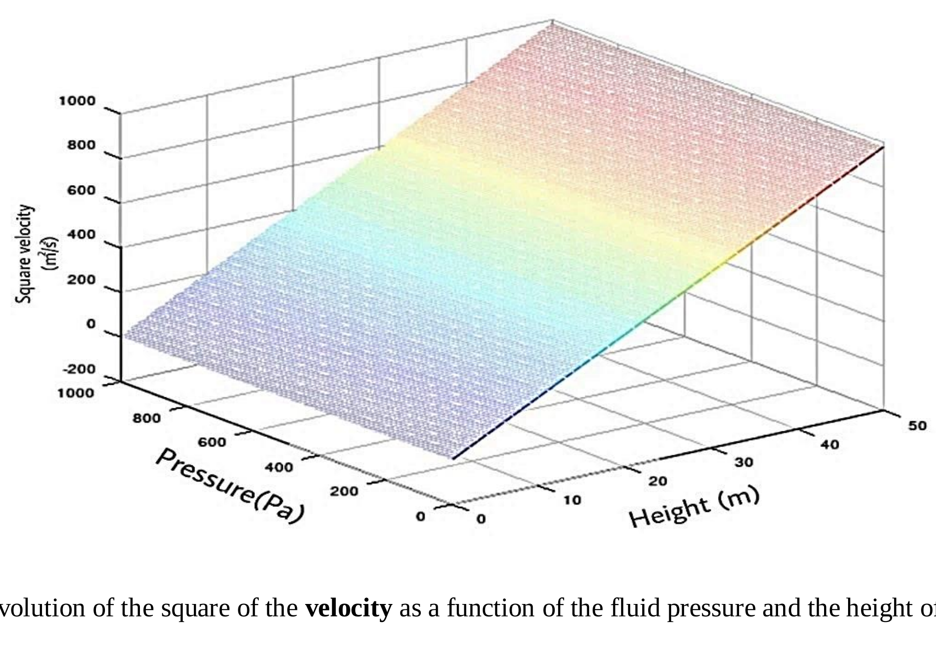

Figure 8: the evolution of the square of the **velocity** as a function of the fluid pressure and the height of the column.

3.2. Discussion:

3.2.1. Study of thermal conduction, heat transfer and thermal resistance in the atmospheric distillation column:

This study shows that vaporized crude oil experiences a drop in temperature (Figures 3 and 4), a decrease in the heat exchanged (Figure 5) but also a very low thermal resistance (Figure 6) when it rises to the head of the column.

Some authors who have done similar studies have made the same observations:

P.P. Singh and D.E Maier [**1**] performed simulations on some baseline values of their study and found that a 10% increase in thermal conductivity caused a 6-8% reduction in the peak thermal gradient, whereas a 20% increase in the heat transfer coefficient caused less than a 2% reduction in the peak thermal gradient. Therefore, thermal conductivity is a more sensitive parameter affecting thermal gradients than heat transfer coefficients. Pandey A. K., Kumar M. [22] concluded in their research that the velocity of nanofluids increases with natural convection parameters, while the temperature profile decreases with increasing the value of these parameters.

Majeed et al. [**23**] considered simultaneously the impact of partial slip and heat transfer in the study of non-Newtonian Casson fluid flows outside of an elastic tube with a given value of heat exchanged, they found that if Casson fluid parameters increase this leads to a decrease in the heat exchanged.

For the temperature drop along the column, Tsung [24**]** studied the effects of transferring the walls by natural convection in a vertical hollow cylinder, he concluded that the convective transfer effects of the walls are not negligible.

The effect of the thermal conductivity of the wall on the conjugate free convection of the flow through a vertical finite wall was studied by Abdennacer [25], he found that the conduction through the wall emanates from a very large free convection with the section of the fluid.

Vasiliev L.L. [4] in his work found that the effective thermal resistance (or thermal conductivity) in a heat-conducting tube is one of the most important parameters and is not constant but as a function of a very large number of variables such as the geometry of the tube, the evaporator and the size of the condenser, the structure of the wick and the fluid in question. The total thermal resistance in a heat-carrying tube is the sum of the resistances caused by conduction through the walls (column envelope), the evaporator source of the vaporized fluid wick, the axial flow of the vapor, condensation, and conduction losses through the walls. The thermal resistance in the condensing tubes is very small or even negligible, simulations have shown that the temperature drops throughout the condenser.

Increasing the volume of air or the volume of vapor in a tube greatly decreases conductive heat transfer [6].

3.2.2. The evolution of the pressure and velocity of the fluid in the column:

The application of the Navier-Stocks equation (21) made it possible to establish the variations in pressure and velocity within the atmospheric distillation column. However, the results have shown through Figure (7) that the pressure of the vaporized crude decreases slightly with increasing flow velocity but increases considerably towards the top of the column. On the other hand, the flow velocity within the cylinder is very little influenced by pressure but increases with the progression of the fluid towards the head of the column.

Indeed, Pandey and Kumar [22] concluded in their research that the velocity of nanofluids increases with natural convection parameters, while the temperature profile decreases with increasing the value of these parameters.

Haibo Jin et al. [26] conclude in their work on mass transfers in columns under high temperature and high pressure that mass transfers in these columns are only affected by gas velocity, temperature, solid particle concentration but weakly by pressure, which justifies the small impact of pressure on flow velocities and mass transfers in the column.

According to Li S. et al. [27], larger columns would help to decrease the operating pressure but slightly increase the impact velocity of the fluid. In addition, in order to have a properly expanded cylinder where losses due to shock waves and shear interactions are negligible, Rokni et al.[28**]** propose that the operating pressure should be adjusted rather than the operating temperature, as they argue that the operating temperature has little effect on the output pressures. But on the other hand, the operating temperature is more efficient than the operating pressure at different output speeds.

Zhang B. et al. [**29]** show that the difference in axial velocity is not significant at different operating pressures, indicating that the velocity of the liquid is not greatly affected by pressure. And the simulation results on the pressure at other apparent gas velocities (0.215; 0.253; 0.317 m/s) are similar by 0.160 m/s.

So, this confirms the small impact of pressure on the increase in velocity in the free flow of a fluid in a cylindrical geometry.

Fang X. et al. [30] conclude that as the length of the tube increases, the pressure drops decrease. But also, that even at high pressure, it is possible to measure the viscosity of gases in tubes with low flow velocities if the high-pressure microdifferential pressure gauge and the microflow meter are used. This shows that the increase in pressure does not necessarily lead to an increase in the flow speed of the fluid.

Ning D. Z. [31**]** states that the hydrodynamic efficiency and air pressure inside the wall of a column increases with increasing vertical duct height and wall thickness.

Wu C. et al.[32] did a study on the interdependence of the flow velocity, temperature, and pressure parameters of a fluid in a column. They conclude that at high surface velocities of gases (turbulent flow regime), the differences in heat transfer coefficients between low and high pressure become smaller compared to the surface velocities of gases at low surface velocities (bubbling flow regime). This means that the flow regime (the velocity) has a greater impact on the heat transfer coefficient, while the pressure has a small impact on the regime and therefore on the heat transfer coefficient in a turbulent regime.

The rise of the vapours in the column is done in a compact way, thus facilitating the individual recovery of the oil cuts in the trays. Indeed, the use of strain rate expressions in cylindrical coordinates shows that all components are zero. The movement of the fluid is thus made in the same way as that of a solid of the same shape; This is why it is referred to as <<block>> or solidifying motion [19].

The little impact of pressure in the evolution of the parameters like velocity and heat exchanges in the column make the engineers use a constant pressure (1 atm) in the distillation process.

4. Conclusion:

The objective of this paper was to physically study the atmospheric distillation system in order to simulate the behaviour of the fluid in order to evaluate heat and mass exchanges and the influence of pressure and flow velocity parameters on these exchanges. This study showed that heat exchange and temperature decrease as you move up to the head of the column in accordance with the principle of atmospheric distillation. In addition, the velocity of the fluid increases considerably towards the head of the column and this increase is weakly related to that of the pressure, which decreases slightly with the flow velocity, but increases considerably with the length of the column.

In the fight against corrosion of industrial equipment, the control of these parameters remains essential. The same goes for the safety aspect in the thermal industries.

References

[1] P. P. Singh, D. E. Maier, “Transient Heat Conduction and Hotspot Development prediction in a flaking Roll with Revolving Heat flux and Convection Boundary Conditions” no. J9802 in JAOCS 78, p 787-792, (2001).

[2] Y. Ootao, T. Akai, and U. Tanigawa, “Three-Dimensional Transient Thermal Stress Analysis of a Nonhomogeneous Hollow Circular Cylinder due to a Moving Heat Source in the Axial Direction”, Journal Thermal Stress 18: p 497-512, (1995).

[3] Y. L. Ding, D.S. When, “Particle migration in a flow of nanoparticle suspensions Powder” Tech 149(2-3), p 84-92, (2005).

[4] Q. Yichao, L. Tao, Z. Jie, “Reasearch on analysis of friction and lubrication characteristics of piston-cylinder system in infernal combustion engines using improved multi-layer thermal resistance model, journal of Engineering Mechanics ans Machinery”, Clausius Scientific Press, Canada, vol 8, Num 4, p 33-43, (2023).

[5] L. L. Vasiliev, “Micro and Miniature heat pipes- Electronic component coolers, Applied Thermal engineering”, 28, p 266-273, (2008).

[6] A.O. Ajibade, A.M. Umar, “Effect of Wall Conduction on steady natural convection couette flowin a vertical chanel”, Meccanica, 56, p 2257-2267, (2021).

[7] A. M. Alkaibi, L. Noam, “Heat and mass transfer resistance analysis of membrane distillation”, journal of membrane science 282 (2006), p 362-369, (2006).

[8] J. Schaaf, V.P. Chilekar, J.R. Ommen, B.F.M. Kuster, J.T. Tinge, J.C. Schouten, “Effect of particle lyophobicity in slurry bubble column at elavated pressure”, Chem. Eng. Sci.62, p 5533-5537, (2007).

[9] V.P. Chilekar, J. Schaaf, B.F.M. Kuster, J.T. Tinge, J.C. Schouten, “Influence of elavated pressure and particle lyophobicity on hydrodynamics gas-liquid mass transfer in slurry in slurry bubble columns”, AIChEJ. 56 (3) 584-596, (2010).

[10] B. Bibi, M. Ashraf, G. Rasool, A. Ilyas, T. Sun, A. Wakif, “Dynamic behaviour of mixed heat transfer among horizontal coaxial fixed pipes at varying temperatures: Efficiency of cylindrical heat sink”, Alexandria Engineering Journal 94, p 44-54, (2024).

[11] A.G. Dixon, B. Partopour, “Computational fluid dynamics for fixed bed reactor design”, Annu. Rev. Chem Biomol. Eng. , 11, 109-130, (2020).

[12] M. Bracconi, M. Ambrosetti, M. Maestri, G. Groppi, E. Tronconi, “A fundamental analysis of the influence of the geometrical properties on the effective thermal conductivity of open-cell foams”, Chem. Eng. Process. Process Intensif., 129, p 181–189, (2018).

[13] P. Ranut, E. Nobile, L. Mancini, “High resolution X-ray microtomography-based CFD simulation for the characterization of flow permeability and effective thermal conductivity of aluminium metal foams”. Exp. Therm. Fluid Sci., 67, p 30–36, (2015).

[14] M. Iasiello, N. Bianco, W.K.S Chiu., V. Naso, “Anisotropic convective heat transfer in open-cell metal foams: Assessment and correlations”. Int. J. Heat Mass Transf., 154, p 119682, (2020).

[15] A. Della Torre, G. Montenegro, A. Onorati, G.Tabor “CFD characterization of pressure drop and heat transfer inside porous substrates”. Energy Procedia, 81, p 836–845, (2015).

[16] C. Sinn, F. Kranz, J. Wentrup, J. Thöming, G.D. Wehinger, G.R. Pesch, “CFD Simulations of Radiative Heat Transport in Open-Cell Foam Catalytic Reactors”. Catalysts, 10, p 716, (2020).

[17] M. Zafari, M. Panjepour, M.D., Emami, M. Meratian, “Microtomography-based numerical simulation of fluid flow and heat transfer in open cell metal foams”. Appl. Therm. Eng., 80, p 347–354, (2015).

[18] Z. Wu, C. Caliot, G. Flamant, Z. Wang, “Numerical simulation of convective heat transfer between air flow and ceramic foams to optimise volumetric solar air receiver performances” Int. J. Heat Mass Transf., 54, p 1527–1537, (2011).

[19] Razza S., Heidig T., Bianchi E., Groppi G., Schwieger W., Tronconi E., Freund H. (2016) Heat transfer performance of structured catalytic reactors packed with metal foam supports: Influence of wall coupling. Catal. Today, 273, p 187–195.

[20] C. Sinn, G.R. Pesch, J. Thöming, L. Kiewidt "Coupled conjugate heat transfer and heat production in open-cell ceramic foams investigated using CFD", Int. J. Heat Mass Transf., 139, p 600–612, (2019).
[21] P. Chassaing "Fluid mechanics, first-course elements". ENSEEIHT, POLYTECH collection of the I. N.P of Toulouse: p 296-300, (1997).
[22] A. K. Pandey, M. Kumar, "Natural convection and thermal radiation influence on nanofluid flow over a stretching cylinder in a porous medium with viscous dissipation", Alexandria Eng. J. P 1-8, (2016).
[23] A. Majeed, T. Javed, A. Ghaffari, M. M. Rashidi, "Analysis of heat transfer due to stretching cylinder with partial slip and prescribed heat flux : a Chebyshev spectral Newton iterative Scheme", Alexandria Eng. J. 54 (4), p 1029-1036, (2015).
[24] Y. N. Tsung "Effect of wall conduction on natural convection over a vertical slender hollow circular cylinder" Appl Sci Res 54, p 39-50, (1995).
[25] B. Abdennacer, B. Smail, A. Said ,"Effect of wall conductivity on conjugate natural convection in a square enclosure with finite vertical wall thickness" Adv Theory Appl Mech 5(4), p 179-190, (2012).
[26] H. Jin, S. Yang, G. He, D. Liu, Z.Tong, J. Zhu, "Gas–Liquid Mass Transfer Characteristics in a Gas–Liquid–Solid Bubble Column under Elevated Pressure and Temperature, chinese Journal of chemical engineering 22, p 955-961, (2014).
[27] S. Li, B. Muddle, M. Jahedi, J. Soria, "A Numerical Investigation of the Cold Spray Process Using Underexpended and overexpanded Jets", J. Therm. Spray Technol., 21, p 108-120, (2012).
[28] M. R. Rokni, S. R. Nutt, C. A. Widener, V. K. Chapagne, R. H. Hrabe "Review of Relationship Between Particle Deformation, Coating Microstructure, and Properties in High-Pressure Cold Spray", J. Therm. Spray Technol , p 1-49", (2017).
[29] B. Zhang, L. Kong, H. Jin, G. He, S. Yang, X. Guo, "CFD simulation of gas-liquid flowin a high-pressure bubble column with a modified population balance model'', Chinese journal of chemical engineering , 26, p 1350-1358, (2018).
[30] X. Fang, X. Yue, Y. Fu. Joseph, A. Weiqin, J. Zou, X. Feng, W. Tian,"Experimental study on factors affecting the end effect in gas viscosity measurement using capillary-tube viscometer", Rev. Sci. Instrum. 90, 074101, p 1-9, (2019).
[31] D. Z. Ning, "Geometrical investigation of a U-shaped oscillating water column wave energy device, Applied Ocean Research" , Elsilver BV, p 1-24, (2020).
[32] C. Wu, M. H. Al-Dahhan, A. Prakash "Heat transfert coefficients in a high-pressure Bubble column, Chemical Engineering Science", vol. 62, no. 1 thru 2, p 140-147, (2007).